Solid Freeform Fabrication 2022: Proceedings of the 33rd Annual International
Solid Freeform Fabrication Symposium – An Additive Manufacturing Conference

POST-PROCESSING VOLUMETRIC ADDITIVE MANUFACTURING (VAM) COMPONENTS

C. S. Kruse*, D. H. Meile*, R. Salajeghe, and J. Spangenberg

Department of Mechanical Engineering, Technical University of Denmark (DTU), Denmark
*These authors contributed equally to this work

Abstract

Volumetric additive manufacturing, a new promising 3D-printing technology, has shown great potential to revolutionize the Additive Manufacturing industry. Within the field of Volumetric Additive Manufacturing, preliminary research has predominantly been focused on improving projection algorithms and optical systems as well as expanding its applicability to different materials, and little attention has therefore been paid to the post-processing phase of the printing process itself. As the surface of components produced by volumetric additive manufacturing using currently available photopolymer and published projection algorithms is not fully cured by the end of projection, it is highly susceptible to damage and deformation in the post-processing phase. In this study, a comparison has been made between the effects of different post-processing methods and techniques on the dimensions of the final post-processed components. The results show that it is a non-trivial task to maintain the surface quality and dimensions of components produced by volumetric additive manufacturing throughout post-processing, and it is therefore important to establish a well-defined method of post-processing that consistently yields satisfactory components.

Introduction

Volumetric additive manufacturing (VAM) is a new and promising field within additive manufacturing (AM) which is capable of printing components on a volumetric basis rather than on a layer-by-layer basis like fused deposition modelling (FDM) [1-3] or stereolithography (SLA) [4], which makes the printing speed orders of magnitude faster. Kelly et al. has been pioneers within the field of volumetric additive manufacturing [5], as they have developed and published the principle behind the volumetric additive manufacturing technique as well as an algorithm capable of generating the intensity-modulated UV light patterns necessary for the technique, named Computed Axial Lithography (CAL) [6], which has been used in this study.

In volumetric additive manufacturing, desired geometries are materialized by projecting intensity-modulated UV light patterns into a rotating cylindrical container filled with a highly viscous and non-linearly hardening photopolymer caused by dissolved oxygen acting as an inhibitor [7]. As the print cylinder rotates, the superposition of the intensity-modulated UV light patterns leads to an accumulated light energy dose within the photopolymer, which causes it to materialize in the shape of the desired geometry after a few minutes of exposure once the inhibiting oxygen has been depleted locally. Upon materialization, the geometries can be taken out of the cylindrical container, and subsequently post-processed and post-cured, to achieve a higher degree of crosslinking.

Due to its significant increase in printing speed, volumetric additive manufacturing has proved itself to be a prominent competitor to current additive manufacturing technologies. One of the challenges of all the additive manufacturing methods is to acquire a part with desired dimensional accuracy [8, 9]. In other vat polymerization techniques, post-processing has shown to play a decisive role in the geometric fidelity and quality of the final components, however this has not yet been given proper attention when it comes to volumetric additive manufacturing. By the end of projection, using the CAL algorithm, the degree of crosslinking for the printed components has shown to be relatively low [7], in contrast to components printed using conventional DLP or SLA printers that uses linearly hardening photopolymers. Because of this, the surface of the printed components is fragile, resulting in it being more susceptible to damage and deformation during post processing, by which removal of the printed components from the cylindrical container and subsequent post-processing must be done carefully. Following the publication by Kelly et al. [7], a new and simplified projection algorithm mitigating this problem was proposed by Rackson et al. [10], which improves the non-linear behavior of the photopolymer and increases the overall degree as well as consistency of crosslinking by the end of projection, however it is not publicly available.

When printed components are taken out of the print cylinder, the surface is covered in a significant amount of residual photopolymer due to the high viscosity. Common to all resin-based additive manufacturing technologies, this residual photopolymer must be removed using a solvent such as isopropanol alcohol (IPA) or tripropylene glycol monomethyl ether (TPM) before the degree of crosslinking can be increased by post-curing using static UV light and heat. However, the method of removing the residual photopolymer varies significantly depending on 3D-printer manufacturer and type of photopolymer used. Some manufacturers sell and recommend using automated washing stations which gently moves the printed components in a back-and-forth motion while it is submerged in a container filled with solvent [11] whereas other manufacturers sell and recommend using ultrasonic cleaners filled with solvent which is more aggressive [12]. Both methods are however intended for post-curing printed components with a high degree of crosslinking, and their applicability to components produced by volumetric additive manufacturing is thus potentially limited due to the nature of the printing process.

Independent of the projection algorithm and the photopolymer type, a well-defined method of post-processing components produced by volumetric additive manufacturing is needed, which can consistently yield satisfactory components with reasonable and predictable geometric tolerances, so that their application is not limited to non-critical cases associated with large geometrical tolerances. In this study, various methods of post-processing components produced by volumetric additive manufacturing has therefore been tested, to investigate how they respectively affect the dimensions of the components, as the first step towards this important factor.

Methodology

To test the applicability of different methods for post-processing components produced by volumetric additive manufacturing, three solid cylinders of equal dimensions were printed using an experimental platform and post-processed using three different procedures. The experimental platform has been designed and constructed at the Technical University of Denmark based on the principles of volumetric additive manufacturing. The three cylinders were printed consecutively using the same intensity-modulated UV light patterns and three identical test tubes with a diameter of 30 mm filled with photopolymer from the same batch, consisting of Bisphenol A glycerolate (1 glycerol/phenol) diacrylate (BPAGDA) mixed with Polyethylene glycol diacrylate (PEGDA) at a ratio of 75:25 wt%. A type 2 photoinitiator system consisting of Camphorquinone (CQ) and Ethyl 4-dimethylaminobenzoate (EDAB) at a ratio of 50:50 wt% was added to the mixture, until the molar concentration of CQ was 5.2 mM - as used by Kelly et al. in their experiments [7]. The projector used for projecting the intensity-modulated UV light patterns was a Wintech PRO4500 with a wavelength of 405 nm and a maximum intensity of 700 mW. The photopolymer overcame inhibition after approximately 3 minutes, after which it was exposed for an additional 30 second before stopping the illumination. The total exposure time for each of the three cylinders was therefore approximately 3 minutes and 30 seconds. In Figure 1, a sketch of the experimental setup can be seen. The test tube was placed in a vat filled with mineral oil acting as a refractive index matched fluid at the focal distance of the projector and rotated using a rotary stage during projection of the intensity-modulated UV light patterns.

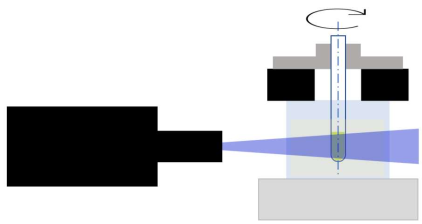

Figure 1: Sketch of experimental setup

Before printing the three cylinders, the dimensions of the projected intensity-modulated UV light patterns were adjusted to be 10x10 mm, to be compliant with the focal depth of the lens mounted on the projector. During crosslinking, the geometry shrinks approximately 10% [7], by which the dimensions of the cylinders are expected to be around 9x9 mm. Due to a small difference in the refractive indices of the mineral oil and photopolymer mixture combined with non-telecentric illumination, the projected UV light patterns are slightly distorted. However, in previous experiments it has been proved that the experimental platform is capable of consistently printing components with an aspect ratio close to the intended aspect ratio of the projected intensity-modulated UV light patterns [13], in this case 1:1. In other words, the distortion is close to being uniform on both axes. After having printed the three cylinders, the procedure for the three post-processing experiments were as follows:

Experiment #1 – Reference

1) The test tube was heated up to reduce the viscosity of the residual photopolymer.
2) The printed cylinder was carefully removed from test tube and transferred to a beaker filled with isopropanol alcohol.
3) The beaker was carefully moved back-and-forth to dissolve the residual photopolymer on the surface of the cylinder with the isopropanol alcohol.
4) The printed cylinder was carefully transferred to a weighing tray and afterwards post-cured

Experiment #2 – Ultrasonic cleaning

1) Test tube was heated up to reduce viscosity of residual photopolymer.
2) Cylinder was carefully removed from test tube and transferred to beaker filled with isopropanol alcohol.
3) Beaker was placed in an ultrasonic cleaner for 3 minutes.
4) Cylinder was carefully transferred to a weighing tray and afterwards post-cured

Experiment #3 – Hot air

1) Test tube was heated up to reduce viscosity of residual photopolymer.
2) Cylinder was carefully removed from test tube and transferred to a weighing tray
3) Cylinder was soaked in isopropanol alcohol while heating it using a heat gun to reduce the viscosity and blow of the dissolved residual photopolymer
4) Cylinder was carefully transferred to a weighing tray and afterwards post-cured

Tests & Results

Upon having prepared the three identical test tubes with the same amount of photopolymer, the three cylinders were printed consecutively using the experimental platform. Below in Figure 2, a timeline of the printing process for one of the cylinders can be seen. The dark spots that can be seen in the pictures are trapped air bubbles from when mixing and pouring the photopolymer, which due to the high viscosity at room temperature has difficulty escaping.

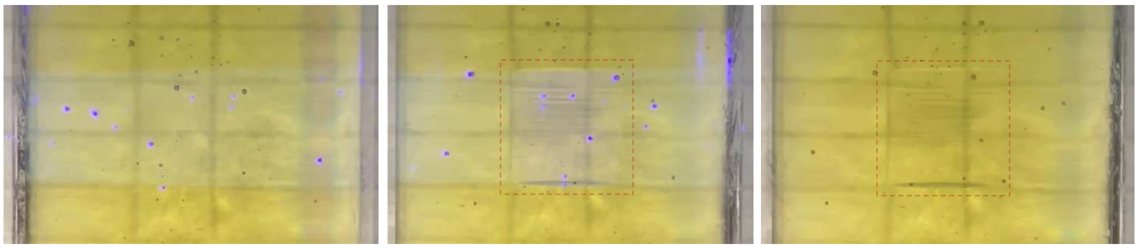

Figure 2: Timeline of printing process *(left: start, center: 3 min 29 sec, right: 3 min 30 sec - projection stopped)*

After having printed the three cylinders, they were each carefully removed from the test tubes and post-processed accordingly, using the three described procedures. In Figure 3, three pictures of the final post-processed cylinders can be seen. The pictures were taken during post-curing using a UV lamp, which is the explanation for the radiant blue color.

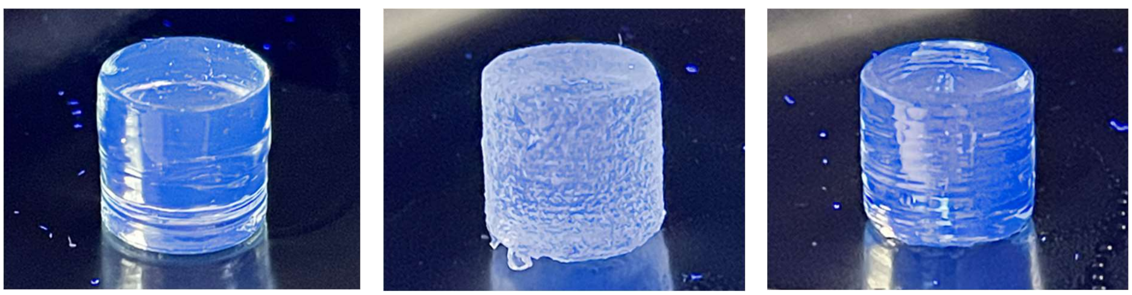

Figure 3: Post-processed cylinders *(left: experiment #1, center: experiment #2, right: experiment #3)*

Once the cylinders were appropriately post-cured, their respective height and diameter were measured using a digital caliper. In Table 1, these measurements together with the calculated aspect ratio and an assessment of the surface quality can be seen.

Experiment	Height	Diameter	Aspect ratio	Surface quality
#1 – Reference	9.13 mm	9.10 mm	1:0.997	Smooth
#2 – Ultrasonic cleaning	8.70 mm	8.55 mm	1:0.983	Pitted
#3 – Hot air	8.65 mm	8.80 mm	1:1.017	Rippled

Table 1: Test results

Discussion

From the test results it can be clearly seen that the three respective post-processing procedures affect the dimensions and surface quality of the three cylinders differently. Most notably, the ultrasonic cleaning post-processing procedure (experiment #2) resulted in a cylinder with significantly smaller dimensions and a pitted surface, however, still with an aspect ratio reasonably close to 1:1. The hot air post-processing procedure (experiment #3) resulted in a cylinder with a smaller height than diameter and a rippled surface, however, also with an aspect ratio reasonably close to 1:1. The reference post-processing procedure (experiment #1) resulted in a cylinder with a similar height and diameter and smooth surface, leading to an aspect ratio that is very close to 1:1. Despite the dimensions not being 10x10 mm due to the aforementioned 10% shrinkage of the material during crosslinking, this shows that the distortion as previously described is close to being uniform on both axes, meaning that the desired dimensions of 10x10 mm could potentially be achieved by scaling the projected intensity-modulated UV light patterns accordingly. This naturally applies to all three cylinders, by which the dimensions of the cylinders in the ultrasonic cleaning and hot air experiments must be evaluated relative to the dimensions of the cylinder in the reference experiment.

The differences in the dimensions of the cylinder in the reference experiment and the cylinders in the ultrasonic cleaning and hot air experiments are believed to be a direct consequence of the non-uniform degree of crosslinking throughout the geometry due to using the CAL algorithm, by which more of the surface having the lowest degree of crosslinking is removed by the more aggressive post-processing procedure. This is especially evident for the cylinder in the ultrasonic cleaning experiment, which is significantly smaller than the cylinder in the reference experiment due to the aggressive nature of ultrasonic cleaning. Additionally, it is also noted that the difference between the height and diameter is larger for the cylinder in the ultrasonic cleaning experiment, resulting in it having a lower aspect ratio. One explanation for this phenomenon could potentially be that the conversion degree is even less for surfaces along the axis of rotation due to the non-uniform accumulated light energy dose, by which more of the curved surface compared to the top and bottom surfaces of the cylinders is removed during post-processing. This would also apply to the cylinder in the reference and hot air experiment, however the cylinder in the hot air experiment, can be observed to have a smaller height than diameter. The cause for this is believed to be using a heat gun rather than a less powerful heat source. In the experiment, the heat gun was oriented perpendicular to the top surface of the cylinder to force the dissolved residual photopolymer on the curved surface downwards - however the temperature of the hot air could potentially have been too high, by which the cylinder was deformed or the top surface damaged.

Overall, it would be interesting to replicate the experiments in this study using the projection algorithm proposed by Rackson et al. [10] and then compare the results to see how it affects the dimensions of the post-processed components, if it becomes publicly available.

Conclusions

From this study it can be concluded that the dimensions of components produced by volumetric additive manufacturing is highly dependent on the uniformity of the conversion degree as well as the post-processing procedure. Ultrasonic cleaning can potentially not be used to post-process components produced by volumetric additive manufacturing unless a higher and more uniform degree of crosslinking is achieved, however, it is still likely that surface pitting is unavoidable due to its aggressive nature unless the degree of crosslinking becomes comparable to that of components printed by conventional resin-based additive manufacturing technologies. Using hot air to reduce the viscosity of the residual photopolymer on the surface is beneficial - however the temperature must not be too high. The same effect could potentially be achieved by heating the isopropanol alcohol prior to washing, which would also result in a more controlled and uniform heat distribution. Because of this, the best post-processing procedure might be the one used in the reference experiment – which is coincidentally also the simplest - however with hot isopropanol alcohol used instead.

References

[1] Vyavahare, S., Teraiya, S., Panghal, D. and Kumar, S. (2020), "Fused deposition modelling: a review", Rapid Prototyping Journal, Vol. 26 No. 1, pp. 176-201. https://doi.org/10.1108/RPJ-04-2019-0106

[2] R. Comminal, M.P. Serdeczny, D.B. Pedersen, J. Spangenberg, Numerical modeling of the strand deposition flow in extrusion-based additive manufacturing, Addit. Manuf. 20 (2018) 68–76. https://doi.org/10.1016/j.addma.2017.12.013.

[3] M.T. Mollah, R. Comminal, M.P. Serdeczny, D.B. Pedersen, J. Spangenberg, Stability and deformations of deposited layers in material extrusion additive manufacturing, Addit. Manuf. 46 (2021). https://doi.org/10.1016/j.addma.2021.102193.

[4] Huang, Jigang. (2020). A Review of Stereolithography: Processes and Systems. Processes. 8. 1138. 10.3390/pr8091138.

[5] Kelly, Brett & Bhattacharya, Indrasen & Shusteff, Maxim & Panas, Robert & Taylor, Hayden & Spadaccini, Christopher. (2017). Computed Axial Lithography (CAL): Toward Single Step 3D Printing of Arbitrary Geometries.

[6] Brett E. Kelly et al. CAL MatLab Software. URL: https://github.com/computed-axial-lithography/CAL-software-Matlab.

[7] Brett E. Kelly et al. “Volumetric additive manufacturing via tomographic reconstruction”. In: Science 363.6431 (2019), pp. 1075–1079. DOI: 10 . 1126 / science.aau7114.

[8] R. Comminal, J.H. Hattel, J. Spangenberg, Numerical Simulations of Planar Extrusion and Fused Filament Fabrication of Non-Newtonian Fluids, Annu. Trans. Nord. Rheol. Soc. (2017). https://nrs.blob.core.windows.net/pdfs/nrspdf-5d42483a-2eeb-43ec-b4ab-a1614ac62f1a.pdf.

[9] M.P. Serdeczny, R. Comminal, D.B. Pedersen, J. Spangenberg, Numerical prediction of the porosity of parts fabricated with fused deposition modeling, Solid Free. Fabr. 2018 Proc. 29th Annu. Int. Solid Free. Fabr. Symp. - An Addit. Manuf. Conf. SFF 2018. (2020) 1849–1854.

[10] Charles M. Rackson, Kyle M. Champley, Joseph T. Toombs, Erika J. Fong, Vishal Bansal, Hayden K. Taylor, Maxim Shusteff, Robert R. McLeod, Object-space optimization of tomographic reconstructions for additive manufacturing. ISSN 2214-8604. https://doi.org/10.1016/j.addma.2021.102367.

[11] https://formlabs.com/post-processing/wash-cure/

[12] https://store.zortrax.com/post-processing/ultrasonic-cleaner

[13] C. S. Kruse, D. H. Meile - Development of a Volumetric Additive Manufacturing machine. Bachelor’s Thesis, Department of Mechanical Engineering, Technical University of Denmark – spring 2021.